2023 NDIA MICHIGAN CHAPTER
GROUND VEHICLE SYSTEMS ENGINEERING
AND TECHNOLOGY SYMPOSIUM
<POWER AND MOBILITY> TECHNICAL SESSION
AUGUST 15-17, 2023 - NOVI, MICHIGAN

A MODEL PREDICTIVE CONTROL-BASED OPERATION OF VEHICLE-BORNE MICROGRID CONSIDERING BATTERY DEGRADATION

Saroj Paudel[1], Jiangfeng Zhang[1], Beshah Ayalew[1],
Matthew Castanier[2], Annette Skowronska[2]
[1] Department of Automotive Engineering, Clemson University, SC, USA
[2] US Army DEVCOM Ground Vehicle Systems Center, Warren, Michigan

ABSTRACT

Microgrids have garnered attention as they facilitate the integration of distributed renewable and non-renewable energy resources and allow flexibility to connect to the grid whenever required. When power is required for temporary missions or an emergency search and rescue mission, a vehicle-borne microgrid can supply critical power needs. In this paper, a vehicle-borne mobile microgrid consisting of a diesel generator, a battery storage system and solar panels mounted on the vehicle exterior is considered, and an operational control that minimizes the total fuel consumption and the battery degradation is formulated based on model predictive control. A simulation study is carried out considering a forward operating base mission scenario where the microgrid supplies the charging power to unmanned ground and aerial vehicles deployed in the mission. The result shows that the proposed approach is robust against uncertainties associated with renewable generation and the charging power demand of unmanned ground and aerial vehicles.

Citation: S. Paudel, J. Zhang, B. Ayalew, M. Castanier, A. Skowronska, "A Model Predictive Control-based Operation of Vehicle-Borne Microgrid Considering Battery Degradation," In *Proceedings of the Ground Vehicle Systems Engineering and Technology Symposium* (GVSETS), NDIA, Novi, MI, Aug. 15-17, 2023.

1. INTRODUCTION

A microgrid (MG) is an integrated system of electricity generation, distribution infrastructure, and some form of energy storage systems to maintain power supply to a certain geographical area [1]. An MG's power rating can range from a few kilowatts to a few megawatts and, in many cases, is connected at a single point called the point of common coupling (PCC) at the distribution level of a commercial utility power system [2]. An MG is powered by micro-sources, which may include renewable sources such as solar panels and wind turbines or non-renewables such as diesel generators and battery storage or hydrogen storage to

collectively meet the load demand. For example, Ref. [3] describes a microgrid that consists of two 1.8MW diesel generators, a 1.5MW/4.5MWh battery storage and a 250kW-15min ultracapacitor pack to supply the Borrego Springs community in the desert area of San Diego County. Ref. [4] describes Ramona Microgrid that provides backup power to the Ramona Air Attack Base, home to CAL FIRE and the US forest service's aerial firefighting assets.

In military applications, a study by the Department of Defense [5] has recognized that autonomous systems, including unmanned aerial vehicles (UAVs), unmanned ground vehicles (UGVs) and unmanned underwater vehicles (UUVs) operating from a forward operating base (FOB) and employing modern intelligence, surveillance, and reconnaissance (ISR) and advanced weapon systems will require an increasing quantity of tactical energy. In this paper, we consider a vehicle-borne mobile microgrid (VBMG) with envisaged applications for the power supply for UAVs and UGVs used during emergencies or in FOB missions. While the UAVs and UGVs come in various sizes and capabilities, we consider battery-powered UAVs and UGVs with a stored energy capacity of approximately a kilowatt-hour or smaller for a UAV and a few kilowatt-hours to a few tens of kilowatt-hours of stored energy for a UGV. A VBMG is often operated in islanded mode due to the nature of the missions except when it is connected to the grid at FOB depots, usually for charging its own battery storage system. The design aspect of such an MG has been discussed in [6] and thus, the focus in this paper will be on the optimal operation of the VBMG. We primarily focus on the economic dispatch problem. Various control methods, including Model Predictive Control (MPC) based methods are mentioned in [7] and [11]. However, neither of the approaches considers battery degradation

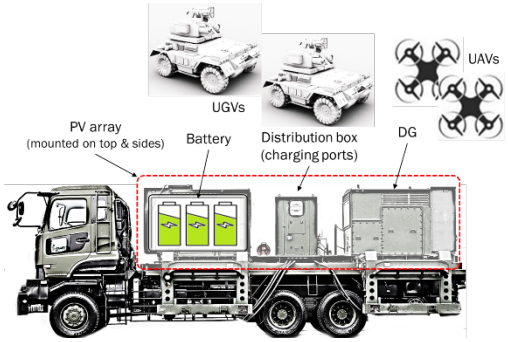

Figure 1: VBMG architecture

models. We propose a model predictive control-based operation considering the fuel consumption and degradation of the batteries.

In section 2, VBMG architecture is briefly described. It is followed by the formulation of the MPC-based operational control of the VBMG and a simulation case study based on the proposed method. Rendezvous planning of UAVs and UGVs with the VBMG and how these are connected for power transfer is out of the scope of this paper.

2. VBMG ARCHITECTURE

A typical VBMG architecture is shown in Figure 1. A diesel generator (DG) and a battery energy storage system (BESS) are housed inside a container mounted onto the trailer, while photovoltaic (PV) panels are mounted on the exterior of the container. A DG is used due to its superior reliability and its power output capability relative to size and cost compared to renewable sources and battery storage. Since the primary purpose of the VBMG is to supply charging power to the UAVs and UGVs deployed in a mission, a distribution box with an ample number of charging ports or pads where the UAVs and

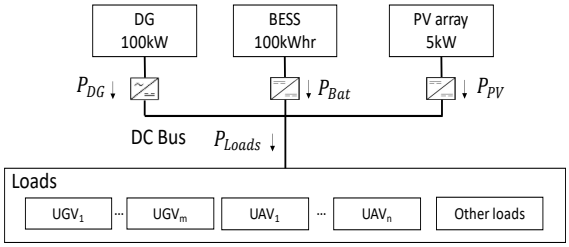

Figure 2: Microgrid load flow model

the UGVs get physically connected to the VBMG is assumed available.

Figure 2 shows the microgrid power flow model. The charging loads are primarily DC, and thus a common DC bus is considered. PV and battery storage system are connected to the DC bus through individual DC-DC converters, while the DG is connected via an AC-DC inverter. During normal operation, the charging load is first supplied by the PV, and the unmet demand is then supplied by the DG and BESS. When there are no loads connected, PV power is directed to battery charging.

2.1. Resources modeling

First, we discuss the constraints on the DG. The output power of DG at any time, $P_{DG}(t)$, is bounded by equation (1), where $P_{DG}^{min}$and P_{DG}^{max} are the minimum and maximum power output of the DG, respectively, and t is the discrete time index. In addition, equation (2) shows the ramping limits of DG. For simplicity, the maximum ramping up and the maximum ramping down limits are assumed identical and represented by R_{DG} . Fuel consumption of DG has been traditionally modeled as quadratic on output power and is given by equation (3), where C_{DG} is the fuel consumed in time Δt and α, β and γ are coefficients[12] . Lastly, due to the operational scenario, there is a limitation in the fuel supply which is represented by equation (4).

$$P_{DG}^{min} \leq P_{DG}(t) \leq P_{DG}^{max} \quad (1)$$

$$|P_{DG}(t) - P_{DG}(t-1)| \leq R_{DG} \quad (2)$$

$$C_{DG}(t) = (\alpha P_{DG}(k)^2 + \beta P_{DG}(k) + \gamma)\Delta t \quad (3)$$

$$\sum_{t=0}^{T} C_{DG}(t) \leq FS \quad (4)$$

Next, we discuss the PV source. PV output, $P_{PV}(t)$ is given by the product of the average PV output ratio, κ, and the maximum PV output, P_{PV}^{max} as shown in equation (5).

$$P_{PV}(t) = \kappa(t) * P_{PV}^{max} \quad (5)$$

Lastly, we discuss the battery storage system. We assume Li-ion battery pack. The power output at time *t*, denoted by $P_{Bat}(t)$, is constrained by battery ratings and is shown in equation (6). Unlike the DG, we assume that the battery can change its output almost instantaneously and thus, no ramping constraints are set. The state of charge at each time, $SOC(t)$, is given by equation (7) where, E_{Bat} is the energy capacity of the battery. This requires that the initial *SOC* is known. It is assumed that the battery power is constant during the time interval Δt. Theoretically, the state of charge may vary from *no charge* (0) to *fully charged* (1). However, considering the battery degradation associated with extreme SOC values, a constraint is added as shown in equation (8).

$$P_{Bat}^{min} \leq P_{Bat}(t) \leq P_{Bat}^{max} \quad (6)$$

$$SOC(t) = SOC(t-1) - \frac{P_{Bat}(t-1)\Delta t}{E_{Bat}} \quad (7)$$

$$SOC^{min} \leq SOC(t) \leq SOC^{max} \quad (8)$$

2.2. SEI *Based battery degradation*

Every battery, including Li-ion battery, is prone to capacity degradation with time and use. Formation and growth of solid electrolyte interface (SEI) in the electrodes is considered to be the most significant life-limiting mechanism in Li-ion battery cells with graphite negative electrodes. SEI layer growth happens in the negative electrode and primarily during charging [8]. This mechanism is associated with side reaction current density j_s which is a function of SOC and current through the cell. Battery degradation is directly proportional to this SEI side reaction current density. Figure 3 shows the plot of j_s against SOC for various charging rates. Degradation is most severe while charging and least severe while discharging. It is noted that degradation during resting (i.e., the battery is idle) is greater than degradation during discharging. For details of this model, readers are referred to [8] and Chapter 7 of [9].

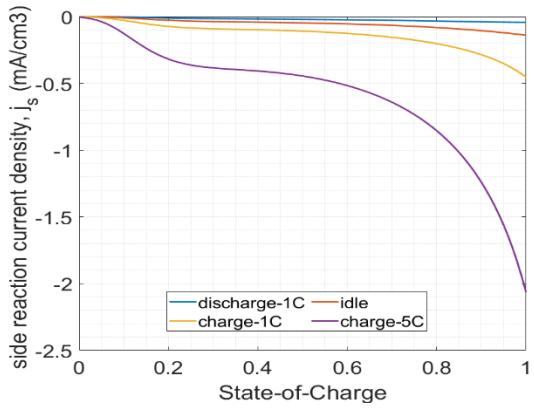

Figure 3: Side reaction current density vs SOC

Considering a battery pack with n modules connected in series and each module consisting of m cells connected in parallel, current through each cell is given by equation (10), where V is the terminal voltage of the cell. For simplicity, V is assumed to be constant and equal to the rated voltage of the cell. The rate of change in capacity of each cell, $\dot{Q}_{cell}(t)$ is then given by equation (11) where a_s, A_s and L_n are cell electrode geometric parameters and F is Faraday's constant. $j_s(t)$ is negative which implies $\dot{Q}_{cell}$ is negative. The capacity loss, Q_{loss}, for the battery pack is then given by equation (12).

$$j_s(t) = f(SOC, i_{cell}) \quad (9)$$

$$i_{cell}(t) = \frac{P_{Bat}(t)}{mV} \quad (10)$$

$$\dot{Q}_{cell}(t) = a_s A_s F L_n \; j_s(t) \quad (11)$$

$$Q_{loss}(t) = mn\, \dot{Q}_{\text{cell}}(\text{t})\Delta t \quad (12)$$

Based on this, the state of health (SOH) of the battery system can be estimated by equation (13) where $n_{cycles}E_{cap}$ is life-time capacity throughput. This requires that the initial SOH be known. SOH decreases monotonically, and without loss of generality, the initial SOH is assumed to be 1 and subsequent values are constrained by equation (14).

$$SOH\,(t) = SOH(t-1) - \frac{Q_{loss}}{n_{cycles}E_{cap}} \quad (13)$$

$$0 \le SOH(t) \le 1 \quad (14)$$

2.3. Loads

The primary purpose of VBMG is to supply charging power to UAVs and UGVs deployed in a mission. Whenever the SOC of a UAV or a UGV is low, they rendezvous with the VBMG for charging. Not all UAVs or UGVs require charging at the same time instant. The total load $P_{Load}(t)$ is approximated by summing the charging power demand of each UAV and UGV. The binary variables $\delta_{UAV,i}(t), \delta_{UGV,j}(t)$ are 1 when the respective UAV or UGV is scheduled to be charging and 0 otherwise.

$$P_{Load}(t) = \sum_{i}^{n_{UAV}} \delta_{UAV,i}(t) P_{UAV,i}(t) + \sum_{j}^{n_{UGV}} \delta_{UGV,j}(t) P_{UGV,j}(t) \quad (15)$$

Lastly, the power balance constraint shown in equation (16) ensures that the charging power demand is always met by the VBMG.

$$P_{DG}(t) + P_{Bat}(t) + P_{PV}(t) = P_{Load}(t) \quad (16)$$

3. MPC-BASED OPERATION OF VBMG

In this section, we formulate an optimization problem to find out the optimal allocation for the power output of DG and battery. The optimization problem can be divided into two subproblems. First is the minimization of the fuel consumption of the DG, and second, the minimization of the cumulative capacity loss of the battery pack making sure that the charging power demand is met. The optimization problem is shown in equation (17). Here ω_1 and ω_2 are weighing coefficients for fuel consumption and capacity loss, respectively. The optimization variables are the power output from the DG and battery.

$$\min_{P_{DG}(t), P_{Bat}(t)} \sum_{t=0}^{T} \omega_1 C_{DG}(t) + \omega_2 Q_{loss}(t)$$
$$subject\ to: (1)\sim(16), \qquad t = 0 \ \ldots \ T \quad (17)$$

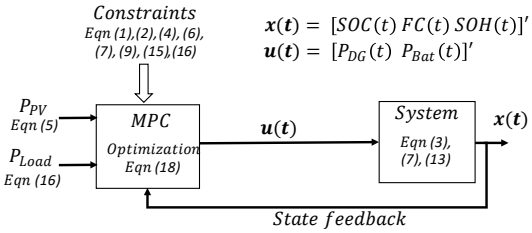

Figure 4: Block diagram of MPC based operation.

where T is the operation horizon for the mission.

An open-loop optimal solution can be easily obtained for this problem. However, the output power of PV connected to the VBMG cannot be accurately predicted for real applications. In addition, the charging power demand for the UAVs and UGVs are also only estimated values at any given time and are continuously updated from higher level mission control. Considering these challenges, an MPC-based operation is appropriate. Figure 4 shows the block diagram of MPC-based operation. MPC uses repeated optimizations with the latest state information and, as such, includes feedback that helps with robustness against changing disturbances or loads (such as PV). This is particularly useful if the load/disturbance sequence for the horizon can be estimated by the VBMG control or demand loads can be communicated to the VBMG control from the UAV/UGV loads to include it in the MPC optimization.

The objective function for closed loop MPC-based operation is obtained from equation (17) by replacing the optimization period with a moving prediction horizon. The problem is rewritten as equation (18) where $[k+1, \dots, k+N_p]$ is the moving prediction horizon of width N_p. This optimization problem is then solved for moving prediction horizons updated every minute.

$$\min_{P_{DG}(t),\, P_{Bat}(t)} \sum_{t=k+1}^{k+N_p} \omega_1 C_{DG}(t) + \omega_2 C_{loss}(t)$$
$$subject\ to: (1) \sim (16), t = k+1 \dots k+N_p \quad (18)$$

Table 1 Simulation Parameters

parameters	*value*	*unit/comment*
P_{PV}^{max}	*5*	*kW*
P_{DG}^{min}	*0*	*kW*
P_{DG}^{max}	*100*	*kW*
R_{DG}	*10*	*kW/min*
FS	*100*	*liters*
a	*1.115e-3*	*liters/kW²*
b	*0.2232*	*liters/kW*
c	*1.75*	*liters*
P_{Bat}^{min}	*-100*	*kW*
P_{Bat}^{max}	*100*	*kW*
E_{Bat}	*100*	*kWh*
SOC^{min}	*0.2*	
SOC^{max}	*0.8*	
$SOC_{initial}$	*0.8*	
$SOH_{initial}$	*1*	
m	*86*	*16 Tesla 6s86p modules in series* $(n = n_1 n_2)$
n_1	*6*	
n_2	*16*	
V	*3.8*	*V*
n_{cycles}	*1500*	

4. SIMULATION CASE STUDY

For the simulation, a mission time of four hours is considered with a time step of one minute. The charging demand at each time step is the aggregated demand of all the UAVs and UGVs at the given time step and is assumed to be known. Simulation parameters are given in Table 1. Cell parameters for degradation modeling are taken from Table 1 in [8]. Simulations are carried out in MATLAB using CasADi [10] framework for formulating the nonlinear optimization problem and the inbuilt open-source IPOPT solver to solve the nonlinear optimization problem. The simulation is run on an Intel Core i7-12700 2.7 GHz PC with 32GB RAM.

First, an open-loop simulation is carried out to find the optimal solution given that the charging demand of the UAVs and UGVs is known beforehand for the whole operational duration (4 hours). Then a model predictive control-based operational plan is simulated

with a prediction horizon of twenty minutes. A random forecasting error (maximum ± 10kW) is introduced at t = 36min.

Figure 5 shows the result of the open-loop simulation. In the open-loop case, all the information is known beforehand, and since the fuel cost is quadratic in the output power of DG, P_{DG} is kept at an optimum level while employing the battery to deal with the unmet demand. However, in the presence of the forecast error (t > 36min), there is a mismatch in the supply and demand. Figure 6 shows the result of the MPC-based operational plan. In the MPC case, the system has information only of the prediction horizon (20 min), the low-cost battery is utilized first, and later, the DG is employed to fulfill the unmet demand. Contrary to the open-loop case, there is no discrepancy between the supply and demand when the disturbance is introduced because the MPC gets updated with the changes at each iteration, thus resulting in a robust operation. It is assumed that there is no forecasting error for the prediction horizon (20 min). It is noted that the forecast error is synthesized data fed to the MPC algorithm, while the source of this error could be either the fluctuations in PV output or the charging load forecast errors or both.

Figure 7 shows the trajectory of the battery's SOC and SOH and the DG's fuel consumption for the open-loop operational plan and MPC-based operational plan. In the open-loop case, the battery is used at around the 20kW power range throughout the operating time, and thus SOC decreases gradually from the initial value to the lower bound value, while in the case of MPC-based operational plan, the battery is used in the beginning and thus SOC falls rapidly and hovers around the lower bound. Battery degradation, represented by SOH, apparently seems to be prominent in the MPC-based operational plan compared to the open-loop case in Figure 7. The difference stems from the fact that in the open-loop case, the

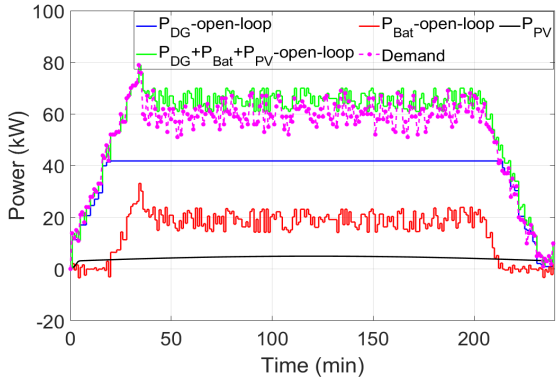

Figure 5: Open-loop operation of VBMG

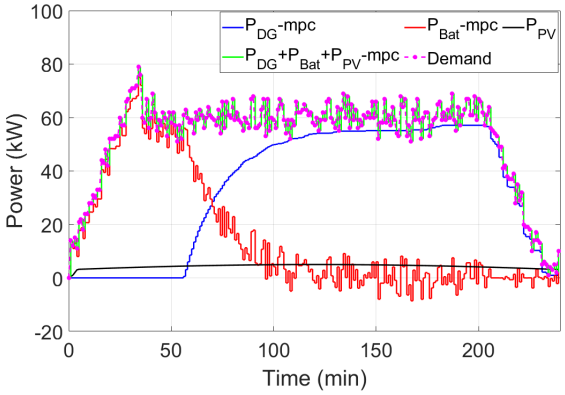

Figure 6: MPC-based operation of VBMG

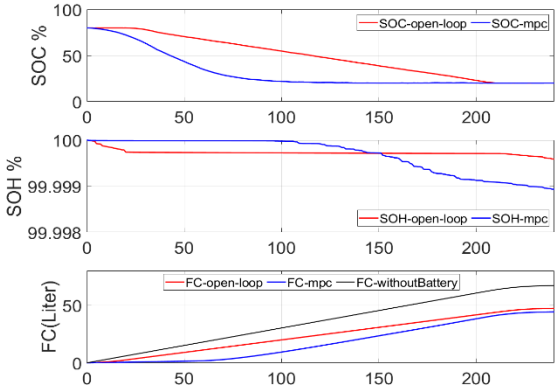

Figure 7: Comparison of open loop and MPC based result for SOC, SOH and fuel consumption.

battery's SOC decreases smoothly throughout the mission time and at only a few instants is the battery being charged, whereas, in the MPC-based operational plan, there are numerous charging instants (when t >100 min), which is when the battery degradation primarily occurs. When we consider the charging period that usually occurs at the charging depot later in the day once the day

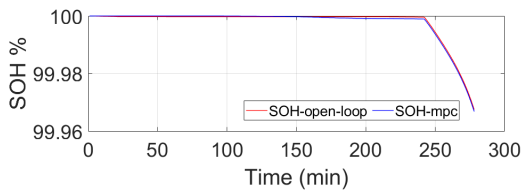

Figure 8: SOH when charging at depot is considered.

mission is over (shown in Figure 8) the degradation during charging is greater than thirty times (when charged at 1C) as compared to the degradation during the discharging period. This is because battery degradation primarily occurs during charging [9][13]. Figure 8 shows that there is no significant difference in the two approaches of operation with respect to degradation over a charge-discharge cycle. However, the difference can become significant for persistent and long-term operations, such as the case of using surveillance UAVs for several days and weeks or months and need further study to compare the two approaches.

Table 2 shows the fuel consumption for three cases. MPC-based operation plan resulted in marginally less fuel consumption as compared to the open-loop case. It is also noted that 6% (12.2kWh) less energy is used to fulfill the charging load demand. The difference is due to the differences between the real-time charging load demand and the forecasted charging load demand that was used to calculate the open-loop solution. However, when the forecasted charging power demand is underestimated and the real-time charging power demand is higher, the MPC-based operational plan may result in higher fuel consumption as it tries to match the higher real-time charging power demand.

The MPC optimization took an average CPU time of 50ms, which is much faster than the update rate of one minute, implying that the proposed method can be implemented for real-time VBMG operational control.

Table 2 Fuel consumption at the end of mission

Simulation Case	FC(Liters)	%change
Open-loop	47.3	-
MPC	44.5	↓ 6%
Without Battery	67.0	↑ 41%

5. CONCLUSION

Based on the simulation case study, it can be inferred that the MPC-based approach provides a feasible approach for the operational control of VBMGs. The inherent robustness of MPC against charging power demand forecasting errors and PV output fluctuations makes it preferable to open-loop operational plans. While battery degradation appears very low for the limited operational durations considered in the case study, it may not be the case for cases where there are numerous charge-discharge cycles involved, such as for supplying UAVs in persistent surveillance applications. In future work, we will consider the stochasticity of PV generation and the charging load. The MPC-based approach will also be further studied with a power-hardware-in-loop (PHIL) system for simulating real mission scenarios.

6. ACKNOWLEDGMENT

This work was supported by Clemson University's Virtual Prototyping of Autonomy Enabled Ground Systems (VIPR-GS), a US Army Center of Excellence for modeling and simulation of ground vehicles, under Cooperative Agreement W56HZV-21-2-0001 with the US Army DEVCOM Ground Vehicle Systems Center (GVSC). Distribution A. Approved for public release; distribution unlimited. (OPSEC 7265)

7. REFERENCES

[1] J. Giraldez, F. Flores-Espino, S. MacAlpine, P. Asmus, "Phase I Microgrid Cost study: Data Collection and Analysis of Microgrid in the United States", Technical Report, October, 2018.

[2] "Microgrid Design Guide", Naval Facilities Engineering Command, December 2016.

[3] A. Pratt, T. Bialek, "Borrego Springs Community Microgrid," International Microgrids Symposium, August, 2019.
[4] https://www.sdgenews.com/article/sdge-completes-ramona-microgrid-partnership-cal-fire-and-us-forest-service (last accessed: Feb. 15, 2023).
[5] "Task Force on Energy Systems for Forward/Remote Operating Bases", Defense Science Board, August 2016.
[6] SB Arshad, J. Zhang, B. Ayalew, P. Pisu, "Optimal power component sizing of vehicle-borne mobile microgrids for military applications", International Conference on Applied Energy, 2020.
[7] T. Pamulapati, M. Cavus, I. Odigwe, A. Allahham, S. Walker, D. Giaouris, "A Review of Microgrid Energy Management Strategies from the Energy Trilemma Perspective", Energies (16) (289), 2023.
[8] A.V. Randall, R.D. Perkins, X. Zhang, G.L. Plett, "Controls Oriented Reduced Order Modeling of SEI Layer Growth", Journal of Power Sources (209), 2012.
[9] G.L. Plett, "Battery Management Systems, Volume II: Equivalent-Circuit Methods", Artech, 2015.
[10] J. Andersson, J. Gillis, G. Horn, J. Rawlings, M. Diehl, "CasADi – A software framework for nonlinear optimization and optimal control", Journal of Mathematical Programming Computation vol. 11, 2018.
[11] H. Wu, X. Liu, M. Ding, "Dynamic economic dispatch of a microgrid: Mathematical models and solution algorithm", International Journal of Electrical Power & Energy Systems, Volume 63, 2014.
[12] M.S. Scioletti, A.M. Newman, J.K. Goodman, A.J. Zolan, S. Leyffer, "Optimal design and dispatch of a system of diesel generators, photovoltaics and batteries for remote locations", Optimization and Engineering 18, 755–792, 2017.
[13] L. Timilsina, P. R. Badr, P. H. Hoang, G. Ozkan, B. Papari and C. S. Edrington, "Battery Degradation in Electric and Hybrid Electric Vehicles: A Survey Study," in IEEE Access, vol. 11, pp. 42431-42462, 2023, doi: 10.1109/ACCESS.2023.3271287.